Spectrochimica Acta Part B 66 (2011) 661–670

Contents lists available at SciVerse ScienceDirect

Spectrochimica Acta Part B

journal homepage: www.elsevier.com/locate/sab

A novel approach to elemental analysis by Laser Induced Breakdown Spectroscopy based on direct correlation between the electron impact excitation cross section and the optical emission intensity

Alessandro De Giacomo *

Department of Chemistry, University of Bari, Via Orabona 4, 70125 Bari, Italy
Institute of Inorganic Methodologies and Plasmas of National Council of Research, Via Amendola 122/D, 70126 Bari, Italy

ARTICLE INFO

Article history:
Received 15 March 2011
Accepted 5 September 2011
Available online 16 September 2011

Keywords:
Excitation cross section
Laser plasma
Laser Induced Breakdown Spectroscopy
Elementary processes
Iron meteorite

ABSTRACT

In Laser Induced Plasma Spectroscopy (LIPS) or Laser Induced Breakdown Spectroscopy (LIBS) the relation between recombining electrons and optical emission intensity has been studied in hydrogen and different metals targets. The role played by the electron impact excitation cross section on the temporal trend of emission lines has addressed and a methodology for the evaluation of the excitation cross sections by optical emission spectroscopy has been tested on several species including H I, Fe I, Ni I, Co I and Ti II. In connection with the theory drawn in this paper, the results show a good agreement with respect to theoretical ones. These results allow the direct linking of the emission intensity to the electronic excitation binary collision. The latter does not depend on experimental conditions and can be applied for elemental analysis. The use of estimated cross sections forms the basis for a different calibration free approach. LIBS elemental analysis on iron meteorites (to be considered as ternary alloys) and on a set of copper based alloys demonstrates the promising use of this analytical approach.

1. Introduction

Laser Induced Plasma Spectroscopy (LIPS) or Laser Induced Breakdown Spectroscopy (LIBS) refers the optical emission of plasma generated by laser-matter interaction, when laser pulses with irradiance around 1 GW cm^{-2} are employed [1]. Emission Spectroscopy is indeed one of the most powerful diagnostic techniques for the investigation of high density ideal plasmas ($N>10^{17}$ cm^{-3}), which is the case of Laser Induced Plasma (LIP) and it allows determining the excitation temperature by using the Boltzmann plot technique [2], the composition [3] and electron number density by Stark broadening [4]. The main assumption for studying plasma parameters is Local Thermal Equilibrium (LTE) [5]. Different criteria can be adopted to justify this assumption in the plasma [6]: when this condition is established, it implies that all the elementary processes involving material particles (electron and heavy particles, i.e. atoms and ions) are balanced while radiative processes, such as spontaneous emission, are not in equilibrium with their backward reactions [7]. On the other hand, in LTE, this deviation in the plasma energy balance is so minor that it does not affect the collisional processes so that all the material particles are characterized by equilibrium distributions in all their degrees of freedom.

In the last decades a strong effort has been directed toward a better clarification of the LTE validity and the development of suitable analytical methods for the investigation of LIP and for the use of LIBS as analytical tool [8–10]. In spite of fast LIBS instrumental development and the increasing interest in studying LIP for various applications in material science, most experimental methodologies have been built in the direction of statistical thermodynamics and macroscopic physical quantities. This paper discusses a novel approach to the interpretation of emission intensity in the plasma based on the use of electron impact excitation cross sections and of the number of electrons subtracted to the plasma by recombination. In this context, the emission is treated as a non-equilibrium phenomenon, as indeed it is, and is interpreted as the decay route of those excitation collisional processes not counterbalanced by superelastic collision. This slight unbalance between the excitation/de-excitation collisional processes is ascribed to the fact that the recombining electrons are characterized by low kinetic energy and so they are mainly involved in the electron impact de-excitation. In this hypothesis the cross section value of excitation electron impact can be estimated by the temporal evolution of LIBS spectra.

The idea of connecting the emission intensity temporal trend and the cross section acquires a fundamental relevance when we realize that the former quantity is strongly dependent on experimental conditions, while the cross section depends only on the species involved in the electron impact excitation binary collision. The prospective of establishing the dependence of emission intensity features in LIP on

* Department of Chemistry, University of Bari, Via Orabona 4, 70125 Bari, Italy. Tel.: +39 080 5929511; fax: +39 080 5449520.
E-mail address: alessandro.degiacomo@ba.imip.cnr.it.

0584-8547/$ – see front matter © 2011 Elsevier B.V. All rights reserved.
doi:10.1016/j.sab.2011.09.003

an absolute quantity, such as the excitation cross section, suggests the possibility of adopting a universal database for fast diagnostics of this kind of plasmas as well as the development of a different approach to calibration-free methodology, as discussed in the last section of the present paper. Last but not least, the estimation of cross sections, as a general topic, is a crucial issue in plasma fundamental research, and the possibility of having at one's disposal an easy tool for its evaluation should indeed be useful to the plasma scientific community.

With the aim of exploring these issues, several previously published experimental data are revisited in this paper and analyzed again with a different approach. In this context, it is essential to stress that, since the laser induced plasma is also strongly inhomogeneous in space, we assume that the different optical systems utilized do not influence the resolved emission data.

2. Experimental set-up

The experimental set-up is a typical LIBS system [8], consisting of Nd: YAG laser sources operating at 10 Hz, 7 ns nominal pulse duration at 1064, 532, 355 nm, a mono-chromator (TRIAX 550 Jobin Yvon with 1800 gr/mm grating) connected to an (ICCD i3000 Jobin Yvon) and a pulse generator (Stanford inc. DG 535) for selecting the delay time and the gate width of the detector. The plasma emission light is imaged by a 7.5 cm focal length biconvex lens directly on the monochromator slit or on the aperture of a fused silica optical fiber. For most of the experiments investigated here, the experimental details have been previously published and the reader is referred to the pertinent references [11–14]. Nevertheless the main experimental features, such as the laser wavelength and fluence, are reported in the present text in order to facilitate its readability.

3. Theoretical considerations

In plasmas with high electron number density ($Ne > 10^{16}\,cm^{-3}$), electrons are expected to thermalize via elastic collisions, with an instantaneous establishment of a Maxwell-like electron energy distribution function (eedf). Nevertheless, this condition is not sufficient to underpin the equilibrium assumption in the plasma. To clarify this point, the effect of the recombination character of the plasma on the eedf can be considered in two opposite cases. The first applies when strong deviations from equilibrium occur because the characteristic times associated with the elastic electron impacts and ion-electron recombination are comparable. In this case, a departure of eedf from the Maxwell distribution is observed for low energy electrons, which in turn results in a considerable overpopulation of high excited levels of heavy particles involved in the recombination processes [9,15] with consequent enhancement of emission intensity from these levels. This scenario generally belongs to weakly ionized, low-density plasmas. In the second case, if the recombination processes proceed slower than elastic electron impacts, the eedf is still Maxwell-like. This means that, whereas slow electrons are lost because of ion-electron recombination, the excess of energy delivered to the heavy particles, involved in the recombination process, is distributed among all the energy levels. This second scenario is that occurring in plasmas with high electron number density in near LTE condition, and it is the one discussed in this paper.

In general, the temporal evolution of the population, N_u, in the upper level u of a species in the plasma is given by:

$$\frac{dN_u}{dt} = N_e N_l k_{lu} - N_e N_u k_{ul} - A_{ul} N_u \tag{1}$$

where N_e is the electron number density, N_l is the population of the species in the lower level l, k_{lu}, k_{ul} and A_{ul} are the rate coefficients of electron impact excitation, de-excitation and spontaneous emission coefficient respectively.

In the Eq. (1) the contribution of the subsequent excitations as well as of the corresponding de-excitation processes linked to the level u have been neglected because the plasma is close to LTE so that those processes are mostly balanced [9]. Note that the effect of metastable levels has been neglected too because of the high density of colliding electrons in the plasma. Here it is assumed that level u can only be populated via collisional process. e.g., the absorption of the continuum emitted by the plasma as well as the contribution to the population of high-excited levels due to the recombination processes, requiring additional terms in Eq. (1), are considered unimportant [9]. This approximation is justified because the contribution of both continuum absorption and recombination to the level population is important only in the early stage of the plasma expansion [16].

In quasi-stationary condition $\frac{dN_u}{dt} = 0$ and so the population N_u is given by the following ratio:

$$N_u = \frac{N_e N_l k_{lu}}{N_e k_{ul} + A_{ul}} \tag{2}$$

Eq. (2) clearly shows that for high electron number density values the collisional term in the denominator prevails over the spontaneous emission coefficient leading to the well-known Mc Whirter criterion for the estimation of LTE condition [6,10].

Eq. (2) can be rearranged as follows:

$$A_{ul} N_u = N_e N_l k_{lu} - N_e N_u k_{ul} \tag{3}$$

Eq. (3) suggests that when the electron impact forward and backward processes are completely balanced, their reaction rates are equal and the emission decay is negligible. More precisely, if excitation/de-excitation rate by electron impact are equal, the only way of depopulation of level *u* is by spontaneous emission which also means that $\frac{dN_u}{dt} \neq 0$, since the radiative processes are not balanced. However, the quasi-stationary-condition still holds since the radiative rates are much less than collisional rates and therefore the emission decay of level *u* is negligible.

Based on Eqs. (2) and (3) it can be stated that the emission contribution strongly depends on the electron number density, N_e, and lower or negligible contribution may be expected for high N_e values.

In the LIP temporal evolution of emission lines, an exponential decay of the intensity is observed because of the decrease of the emitters number density and, to a lesser extent, of the excitation temperature during the expansion [11]. On the other hand, the temporal trend of electron number density is similar to that of the emission lines, with a fast decrease at the beginning of the temporal evolution, as a result of recombination and expansion [5,6,11]. As an example, Fig. 1 reports the temporal evolution of the second Balmer line at 486 nm and the corresponding electron number density (calculated by the same spectral line broadening) in a 150 Torr hydrogen LIP. While the effect of the expansion is the same for all the particles in the plasma (electrons and heavy particles), recombination processes involve only slow electrons [9,17,18]. In Fig. 2 it is shown the cross section energy function of three-body [17] and radiative recombination [18] in the case of hydrogen. By the inspection of Fig. 2 it can be noted that these processes are due almost entirely to electrons with energy below $5000\,cm^{-1}$ (0.62 eV) and, in the energy range $0–5000\,cm^{-1}$, the cross sections decrease more than two orders of magnitude. That means that these recombining electrons do not affect markedly the excitation processes as their energy is below the energy threshold of the excitation transitions involving the most populated levels in any atomic system. On the contrary slow electrons are extremely important for what concerns super-elastic (quenching) collisions. It is reasonable to suppose that the exit of slow electrons from the system as a consequence of recombination processes, prevents electron impact de-excitation to completely balance the excitation processes induced by the fast electrons. To clarify this concept a qualitative scheme is reported in Fig. 3.

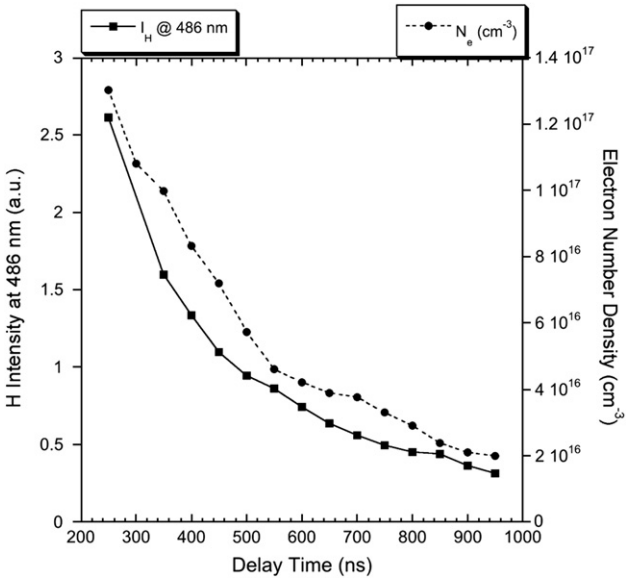

Fig. 1. Temporal evolution of H I Balmer line at 486 nm (■) and of electron number density (●) during LIBS in pure Hydrogen gas at 150 Torr [15]. Gate width 50 ns, delay step 50 ns, laser pulse at 1064 nm with E = 800 mJ focused by 30 cm focal length lens.

In this connection, considering a time interval Δt, the electron impact excitation induced by the electron number density N_e^{t0} at time t_0 is backwarded by the de-excitation electron impact induced by a lower electron number density N_e^{t1} at time t1 = t0 + Δt. Keeping in mind this observations, Eq. (3) can be re-written as:

$$N_u A_{ul} = N_e^{to} N_l k_{lu} - N_e^{t1} N_u k_{ul} = N_e^{t1} N_u k_{ul} \left(\frac{N_e^{to} N_l k_{lu}}{N_e^{t1} N_u k_{ul}} - 1 \right) \quad (4)$$

If the considered time interval Δt is short enough, a linear electron number density decay can be assumed. In this case, the electron number densities at t0 and t1 are linked by the following expression:

$$N_e^{t0} = N_e^{t1} - \Delta N_e \quad (5)$$

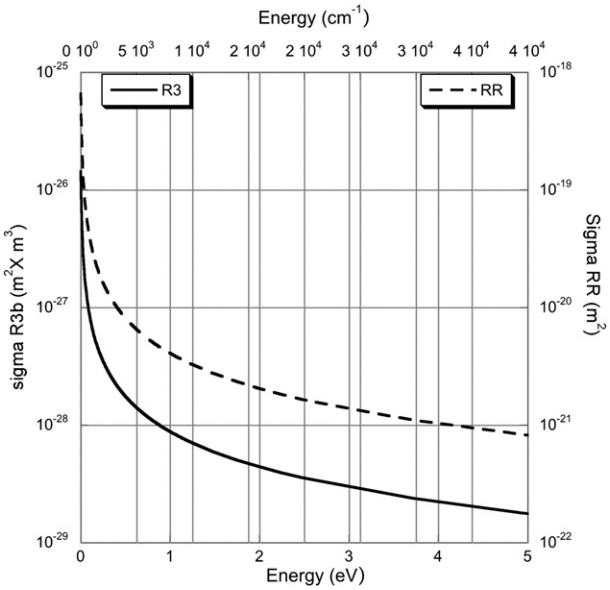

Fig. 2. Three body (R3b) and radiative (RR) electron-ion recombination cross sections as function of the electron energy calculated as shown in Refs.[17,18], respectively.

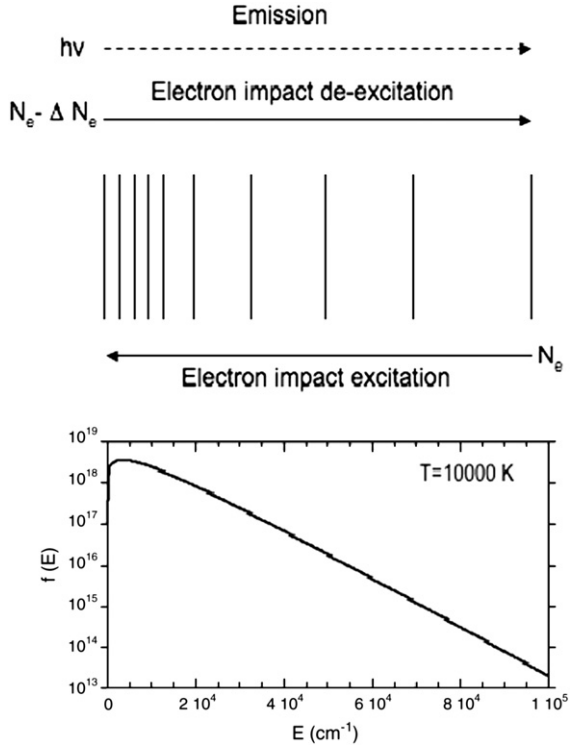

Fig. 3. Scheme of elementary processes balance in LIP. The following processes are considered: Electron impact excitation: $A_l + e^-_{fast} \xrightarrow{k_{lu}} A_u + e^-_{slow}$; Electron impact de-excitation: $A_u + e^-_{slow} \xrightarrow{k_{ul}} A_l + e^-_{fast}$; Spontaneous emission: $A_u \xrightarrow{A_{ul}} A_l + h\nu_{ul}$; Three body recombination: $A^+ + e^-_{slow} + e^- \xrightarrow{k_{R3b}} A + e^-$; Radiative recombination: $A^+ + e^-_{slow} \xrightarrow{k_{RR}} A + h\nu$; The figure shows that, as a consequence of the amount ΔN_e of recombining slow electrons, the electron impact excitation processes is partially counterbalanced by the spontaneous emission.

where $\Delta N_e < 0$, because the plasma is recombining [5,6]. Combining Eq. (5) and Eq. (4) the following equation is obtained:

$$N_u A_{ul} = N_e^{t1} N_u k_{ul} \left(\frac{N_e^{t1} N_l k_{lu}}{N_e^{t1} N_u k_{ul}} - \frac{\Delta N_e N_l k_{lu}}{N_e^{t1} N_u k_{ul}} - 1 \right) \quad (6)$$

If the system is close to LTE and the Mc Whirter criterion is valid (and generally happens in the case of LIP for microseconds time scale) the reaction rates of excitation and de-excitation induced by the same electron number density are equal (and in any case closely similar), i.e.:

$$\frac{N_e^{t1} N_l k_{lu}}{N_e^{t1} N_u k_{ul}} \approx 1 \quad (7)$$

In this hypothesis Eq. (6) leads to the following expression, which correlates directly the number of radiative emissions per unit volume per unit time to the number density of electrons consumed by recombination per unit time:

$$N_u A_{ul} = -\Delta N_e N_l k_{lu} = |\Delta N_e| N_l k_{lu} \quad (8)$$

Eq. (8) establishes the link between the emission intensity of atomic and ionic transitions and the recombining electrons. Moreover the overall discussion above, suggests that the number of optical transitions in the LIP near LTE condition is essentially proportional to the number of electrons disappearing because of recombination.

Note that, in this discussion, the effect of chemical reactions (e.g. molecular formation and dissociation) [19] on the population of excited levels has not been considered here because, it is reasonable to assume that, the LIP is composed essentially by atomic particles at least in the temporal windows useful for LIBS (0.2–10 μs). On the contrary, this effect should play a role in the case of LIP at really long delay time from the laser pulse [11] and in the case of other kind of transient and stationary plasmas [19].

3.1. Estimation of electron impact excitation cross section

The above discussion introduces the possibility to find the correspondence between the statistic approach of emission spectroscopy and the elementary processes occurring in the plasma, namely binary collision between electron and heavy particle. The key of this linking is the electron impact excitation cross section. The latter depends just on the specific particles involved in a single collision and so it does not depend on experimental conditions and can be used to study the system with a "state to state" approach.

Introducing the optical emission intensity [20] in the first member of Eq. (8) the following expression is obtained:

$$A_{ul}N_u = |\Delta N_e|N_l k_{lu} \Rightarrow \frac{4\pi I_{ul}}{h\nu G} = |\Delta N_e|N_l k_{lu} \tag{9}$$

where G is the experimental factor depending on the sampled plasma volume and on the total efficiency of the detection system.

The rate coefficient of an elementary process is given by the following expression [5,7,9], here expressed in terms of the electron impact excitation cross section:

$$k_{lu} = \int_{E_{ul}}^{\infty} f(E)\sigma_{lu}v(E)dE \tag{10}$$

where f(E) is the Maxwell eedf and v(E) is the electron velocity. Combining Eqs. (9) and (10)

$$\frac{4\pi I_{ul}}{h\nu_{ul}G} = |\Delta N_e|N_l \int_{E_{ul}}^{\infty} f(E)\sigma_{lu}v(E)dE. \tag{11}$$

Obviously, the cross section is a function of energy and cannot be determined by a single experimental data such as the emission intensity, without making some assumption that justify neglecting such energy dependence.

In this paper two different assumptions have been tested:

a. The threshold value is considered the most representative value of the cross section. Thus the integral of Eq. (10) assumes the value of the function at the threshold energy E_{ul} and Eq. (11) becomes:

$$\frac{4\pi I_{ul}}{h\nu_{ul}G} = |\Delta N_e|N_l f(E_{ul})\sigma_{lu}^{th}v(E_{ul}). \tag{12}$$

ΔN_e is calculated as the difference between the electron number density values obtained by Stark broadening at different delay times, chosen as close as possible.
The N_l population, unless the G factor, can be recovered by the experimental Boltzmann plot remembering:

$$\ln\left(\frac{N_l}{G}\right) = -\frac{E_l}{kT} + q \tag{13}$$

where q depends on the species concentration N_0 and on the partition function. Note, anyway, that the calculation of N_l to be introduced in Eq. (12) does not require the absolute value of the intercept because the measured emission intensity is yet scaled to the same factor G.

Finally plotting directly the measured intensity I_{ul} vs $|\Delta N_e|N_l f(E_{ul})$ $h\nu_{ul}/4\pi$ at different delay times a line is obtained and the correspondent slope m is:

$$m = \sigma_{lu}^{th}v(E_{ul}) \Rightarrow \sigma_{lu}^{th} = m\left(\sqrt{\frac{2E_{ul}}{m_e}}\right)^{-1} \tag{14}$$

b. The cross section is considered to be constant in all the energy range above the threshold. In this case the cross section can be approximate to a "step function" and the Eq. (11) becomes:

$$\frac{4\pi I_{ul}}{h\nu_{ul}G} = |\Delta N_e|N_l\overline{\sigma}_{lu}\langle v\rangle \exp\left(-\frac{E_{ul}}{kT}\right) \tag{15}$$

By plotting now I_{ul} vs $|\Delta N_e|N_l\langle v\rangle \exp\left(-\frac{E_{ul}}{kT}\right)h\nu_{ul}/4\pi$, at any selected delay time in the interval of observation, the average cross section is directly obtained.

In the next section the difference between these approximations will be discussed for a LIBS experiment performed with Hydrogen. The choice of Hydrogen is dictated by the fact that it is one of the few species for which excitation cross section data are known with a good accuracy. In any case, it is important to underline that this procedure does not claim to determine the excitation cross section, since this parameters, as said before, is a function of energy. Nevertheless it provides useful estimate of the rate at which the excited levels are populated.

4. Experimental

4.1. Hydrogen test case

Pure Hydrogen gas at 150 Torr has been irradiated with 1064 nm laser pulse (pulse energy 800 mJ, repetition rate 20 Hz) focused in the vacuum chamber by a 30 cm focal length lens. The spectra have been collected every 50 ns with a gate width of 50 ns, in the time range from 250 ns to 1000 ns after the laser pulse. The experimental spectra have been shown in a previous work [16]. The electron number density has been calculated by the Stark effect on the line at 486 nm using the data reported in Ref.[21]. A typical Boltzmann plot of H I species as obtained in this experiment is shown in Fig. 4 A, while Fig. 4 B reports the temporal evolution of the excitation temperature obtained by the Boltzmann plot technique. The methods for the estimation of the electron impact excitation cross section described in the previous section have been applied to the temporal evolution of the first four Balmer lines.

Fig. 5 A and B shows the plots of Eqs. (12) and (15), respectively, along the LIP temporal evolution (250–1000 ns). It can be noted that in both cases the curve has a good linearity in agreement with what was expected from the discussion of Section 3.1. The experimentally determined cross section values, as well as the cross section as function of energy taken from Ref.[22], are reported in Fig. 6. By the inspection of Fig. 6, in the case of literature data, it is clear that the dependence of the cross section on electrons energy is indeed not negligible. The cross section value obtained by the experimental estimation, which approximates the cross section to its value at the threshold energy (Eq. 12), appears a reasonable representation of the cross section in the energy ranges typical for electrons in LIP (E<13 eV). Though Eq. (15) is based on a better assumption than Eq. (12), it gives a worse representation of cross section values in the energy range useful for LIBS, because the step function averages the cross section function along all the energy range. In the frame of these observation, Eq. (12) has been preferred as a reference of the excitation cross sections for all the other examples reported in the present paper.

Fig. 7 A–C report plots obtained using Eq. (12), for delay times from 250 to 1000 ns, for the transitions at 486 nm (2–4), 434 nm (2–5) and 410 nm (2–6). The other transitions of the Balmer series are detectable at delay times at which the electron number density does not fulfill the

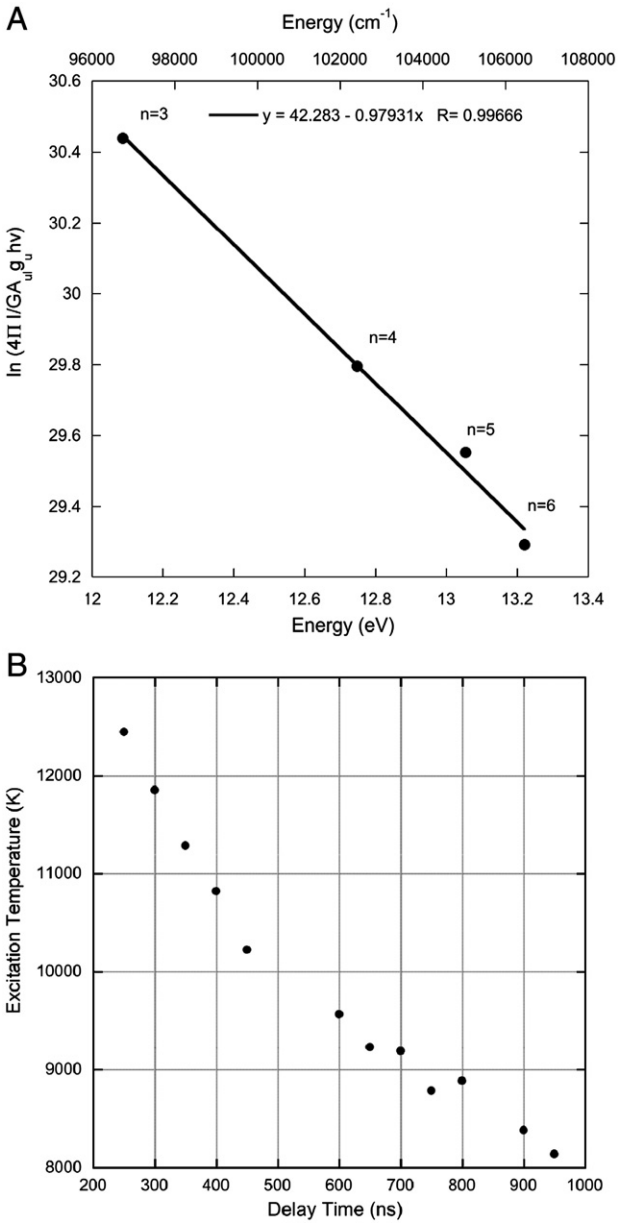

Fig. 4. Boltzmann analysis of 150 Torr hydrogen LIBS: A) typical Boltzmann plot of H I and B) temporal evolution of excitation temperature determined by the Boltzmann plot technique. Gate width 50 ns, delay step 50 ns, laser pulse at 1064 nm with E = 800 mJ focused by 30 cm focal length lens.

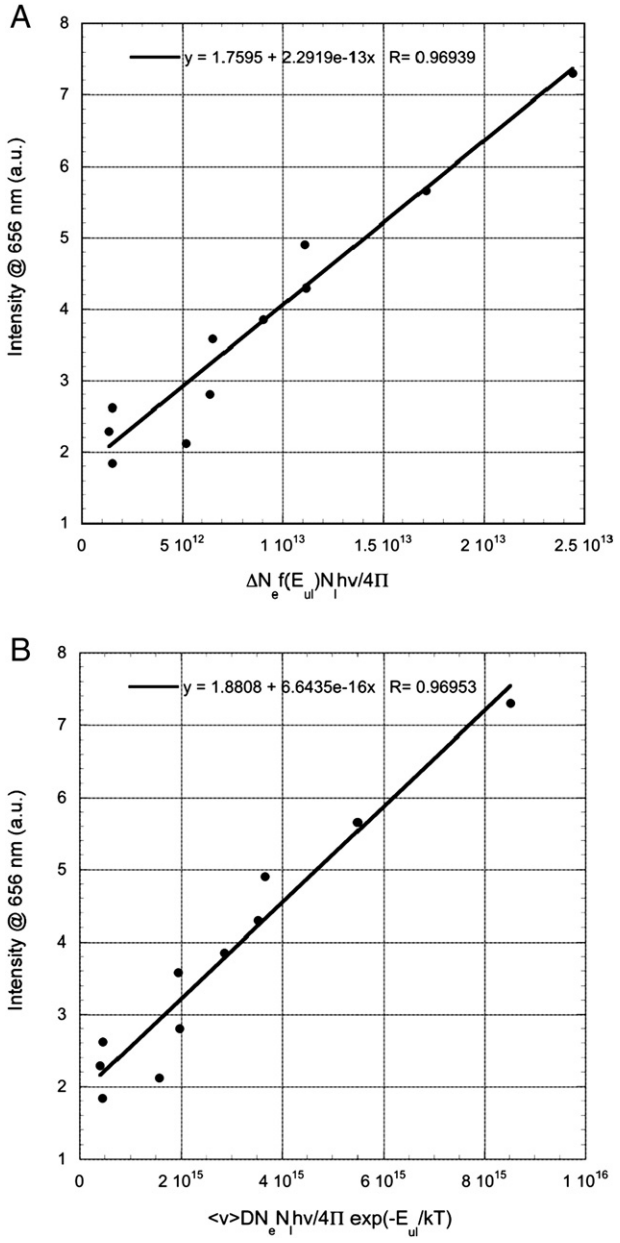

Fig. 5. Experimental plots of A) Eq. (12) and B) Eq. (15) for the Balmer line at 656 nm corresponding, in the plot, to the transition 2–3 in Hydrogen LIBS.

Mc Whirter criterion at the experimental conditions relevant here [6,16]. The resulting LIBS experimental cross section values reported in Table 1 together with the maximum and average values of literature cross section functions [22] show a good agreement.

Once the excitation cross section has been estimated, some relevant information about the time connected to the elementary processes can be inferred, calculating the characteristic time of electron impact excitation, emission and total three body recombination. The experimental time for the excitation has been estimated as the inverse of the slope of graphs reported in Fig. 5 A divided by the fraction of electron with suitable energy in the plasma, for the first Balmer transition, applying the following formula [6, 20]:

$$t_{exc2-3} = \frac{1}{\sigma_{lu}\langle v\rangle N_e \exp\left(-\frac{E_{lu}}{kT}\right)} \tag{16a}$$

The recombination time has been estimated from the value of the three body recombination rate coefficient reported in Ref. [17] with the following equation:

$$t_{R3b} = \frac{1}{k_{R3b}N_e{}^2} \tag{16b}$$

The estimated times are in the order of $t_{exc2\text{-}3} \leq 10^{-9}$ s, $t_{R3b} \geq 10^{-8}$ s and the $t_{hv} \sim 10^{-8}$ s. This result suggests that the time required by the system for the excitation processes to take place is always one order of magnitude smaller than the spontaneous emission time, while the latter is comparable or shorter than the recombination time. In agreement with Refs. [6,23], it would be correct to say that, in the case of 1–2 transition, indeed not detectable in UV–vis spectral range, a longer time should be found for the collisional excitation, so that this scenario holds for a narrower range along the N_e temporal evolution.

The estimated times suggest that for that part of the plasma not in equilibrium, involved with the departure of slow electrons (estimated

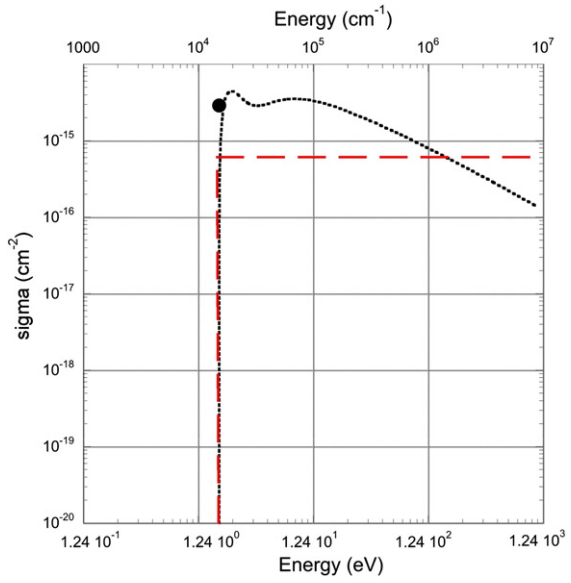

Fig. 6. Electron impact excitation cross section as function of energy (dotted curve) obtained by Ref. [22] and cross section values estimated by Eq. (14) (●) and by Eq. (15) (dashed curve).

to be around 10–5% of the total electron number density by $\Delta N_e/N_e$ X 100), the relaxation time corresponds to the reciprocal of the emission coefficient. With this observation, it could be interesting to note that, whereas a non-equilibrium effect is directly measured by LIP optical emission, the Boltzmann distribution of the emitting species is still observed as a consequence of fast electron impact processes. In other words, it would appear that, when the ion-electron recombination is the "bottleneck" of the kinetic processes, the missing decay of superelestic collisions is replaced by emission.

4.2. Metals test case

The previously discussed procedure for the determination of electron impact excitation cross section has been applied to a set of transitions observed with metal targets in order to test the suitability of the proposed methodology.

The LIP emission obtained by a 355 nm laser pulse, of fluence 15 J cm^{-2}, focussed on an iron meteorite, named Sikhote Alin, with delay time step of 50 ns and gate width of 50 ns has been used as a main example for this purpose.

The plots of Eq. (12) at different delay times for the Fe I lines at 340.74 and 347.67 nm and Ni I at 341.47 nm are reported, as examples, in Fig. 8 A–C. Once again the excellent linearity of Eq. (12) can be clearly seen.

The electron impact excitation cross section of metals, for most elements, are not tabulated, and are not easily found in the literature. In the case of optically allowed transitions, we can refer to some semi-empirical formula as that proposed in Ref. [20]:

$$\sigma_{lu} = \frac{8\pi^2}{\sqrt{3}} a_0^2 f_{lu} \frac{E_H^2}{E_{lu} E} \bar{g} \approx \frac{8\pi^2}{\sqrt{3}} a_0^2 f_{lu} \frac{E_H^2}{E_{lu}^2} \tag{17}$$

Eq. (17) has been rearranged to obtain the maximum cross section value at the threshold energy for a better comparison with the experimental results. The average Gaunt factor has been supposed to be $\bar{g} = 1$, because, generally, in the case of metals emission in

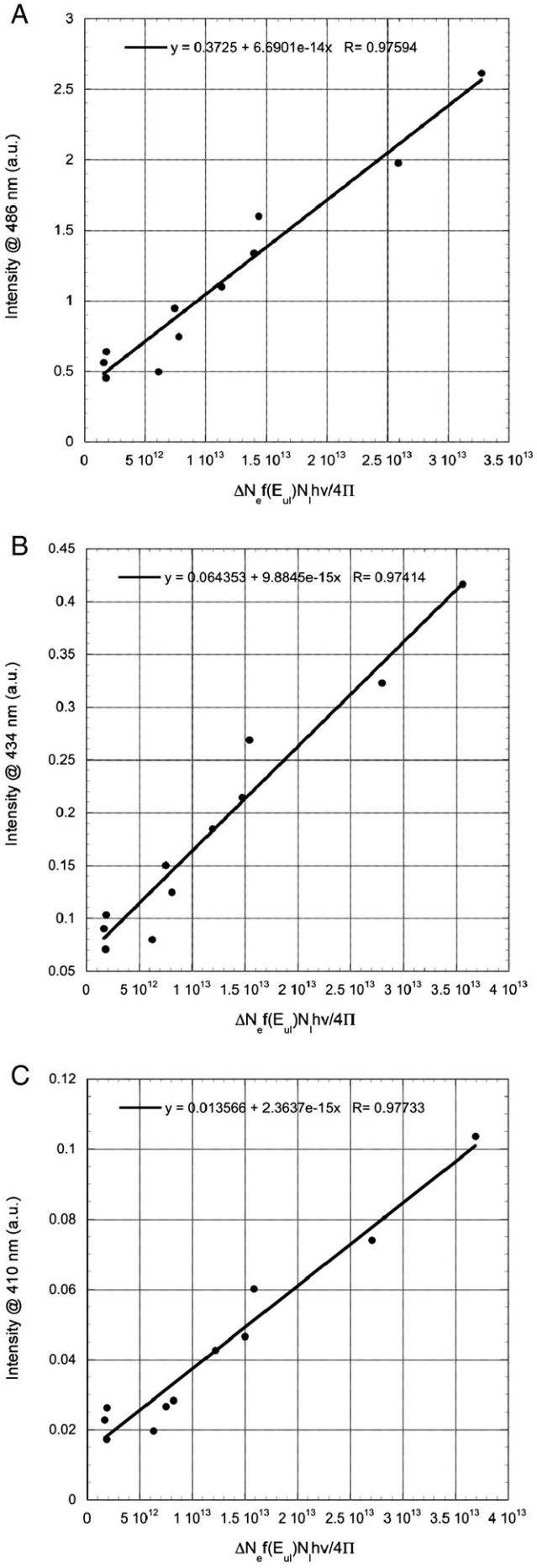

Fig. 7. Experimental plots of Eq. (12) of the Balmer lines at A) 486, B) 434 and C) 410 nm corresponding, in the plot, to the excitation transitions 2–4, 2–5 and 2–6, respectively, in Hydrogen LIBS.

Table 1
Electron impact excitation cross sections of the first four Balmer transitions: in the second column the experimental values are estimated by Eq. (14) for the Hydrogen LIBS experiment, while in the next columns are reported, respectively, the maximum value, the mean values up to the ionization energy E_i, and the mean value along all the energy scale of the cross section energy function taken from Ref. [22].

Balmer transition	σ_{exp} (cm^2)	σ_{max} (cm^2)	$\overline{\sigma}_{E<Ei}$ (cm^2)	$\overline{\sigma}_{E=\infty}$ (cm^2)
656 nm (2–3)	2.82E−15	4.43E−15	2.90E−15	4.21E−16
486 nm (2–4)	7.07E−16	7.57E−16	5,62E−16	7.32E−17
434 nm (2–5)	1.00E−16	2.78E−16	2.01E−16	2.65E−17
410 nm (2–6)	2.36E−17	1.36E−16	9.70E−17	1.29E−17

the UV–vis range, transitions between levels with the same principal quantum number occur [20]. The oscillator strength f_{ul} are available in databases [24, 25]. The other parameters in the equations are the Bohr radius a_0, the H ionization energy E_H and the electron energy E.

Table 2a and 2b report experimental electron impact excitation cross section of different species at different conditions and the theoretical value obtained by Eq. (17). Comparing the values reported in Table 2a and 2b, a good agreement between the experimental and calculated results can be seen. It can be also interesting to note that, in agreement with theory, for transitions between higher excited states, a larger cross section is obtained. In the case of titanium ions (Table 2b) the cross section measurements have been carried out by using single and double pulse experiments described in details in Ref. [11]. Similar values have been obtained, especially keeping in mind that an experimental error (mainly due to the Stark broadening measurements [26]) around 35% should be considered in this case.

4.3. Electron impact excitation cross section: implications to LIBS elemental Analysis

The possibility of knowing the excitation cross section allows performing chemical analysis without the requirement of standard samples, if the ablation processes can be considered stoichiometric. It should be anticipated that the present section does not include the critical discussion on the analytical performance of this methodology because such topic will be addressed in another paper. The aim of this section is just to discuss the potential application of a state to state approach to the LIBS quantitative analysis.

Let us consider as a first step a binary sample composed by the elements X and Y, so that, in agreement with the discussion in section 3.1, for each emission line the following expression can be written:

$$\frac{4\pi I_{ul}}{h\nu_{ul}G} = \Delta N_e f(E_{ul})\sigma_{lu}v(E_{ul})N_l = \Delta N_e f(E_{ul})\sigma_{lu}v(E_{ul})\frac{g_l N_0 \exp\left(-\frac{E_l}{kT}\right)}{Z(T)} \quad (18)$$

Eq. (18) has been arranged inserting the Boltzmann distribution, where N_0 is the number density of the species and Z(T) is the corresponding partition function. Taking the ratio between emission lines of X and Y, respectively, and rearranging the members of Eq. (18) we obtain the following equation:

$$\frac{N_0^X}{N_0^Y} = \frac{I_{ul}^X \lambda_{ul}^X \sigma_{l'u'}^Y v(E_{u'l'}) g_{l'}^Y Z^X(T)}{I_{u'l'}^Y \lambda_{u'l'}^Y \sigma_{lu}^X v(E_{ul}) g_l^X Z^Y(T)} \exp\left(-\frac{E_{l'}-E_l}{kT}\right) \quad (19)$$

It is important to note that in the case of lower levels involved in visible transition in LIBS, it is usual to find emission lines for which the condition $E_{l'} - E_l \ll kT$ holds.

Moreover, this condition is more likely to occur to be found with lower levels than with upper levels, when similar energy values could result in

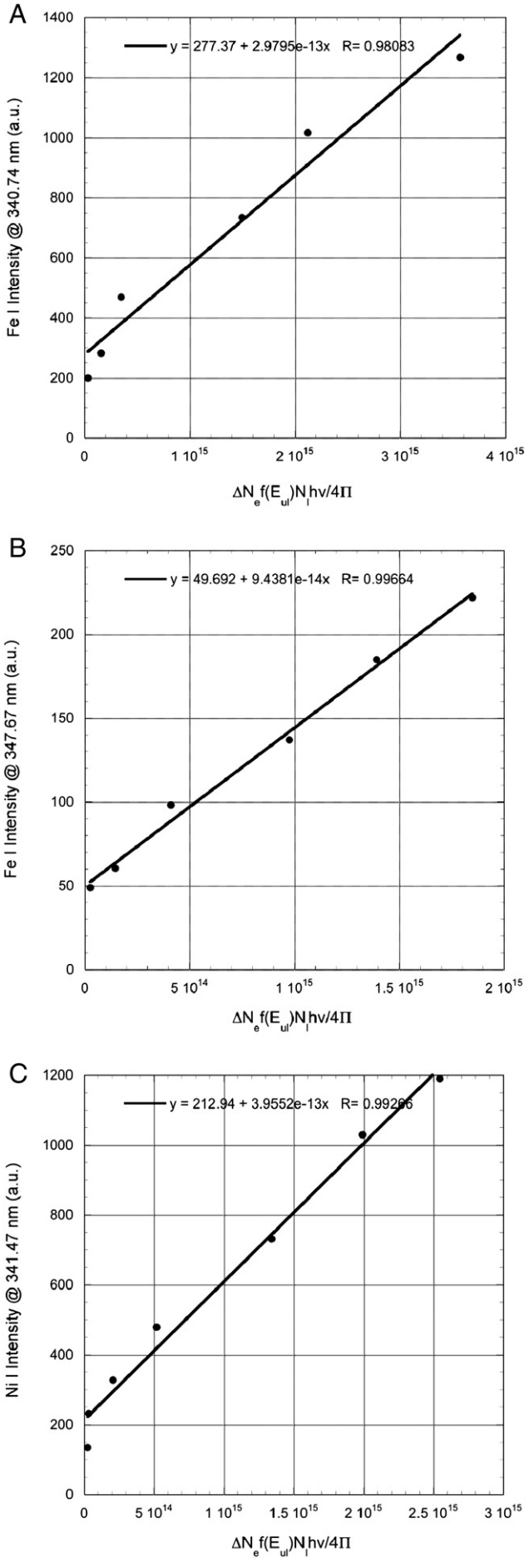

Fig. 8. Experimental plots of Eq. (12) of the emission lines of A) Fe I at 340.74 nm, B) Fe I at 347.67 nm and C) Ni I at 341.47 nm during LIBS on Sikote Alin. Gate width 50 ns, delay step 50 ns, laser pulse at 355 nm with fluence of 15 J cm^{-2}.

Table 2a
Estimated electron impact excitation cross section values of different elements in: a) LIBS experiment on Sikote Alin (delay time step of 50 ns, gate width of 50 ns, laser pulse at 355 nm, fluence 3 J cm^{-2}); b) Single and Double Pulse LIBS on metallic titanium (experimental details can be found in Ref. [11]).

	configurations	E_l (cm^{-1})	E_u (cm^{-1})	σ_{exp} (cm^2)	σ_{cal} (cm^2)
Fe@340.74	3 d^7(^{4}P)4 s -3 d^6(^{3} F2) 4s4p(^{3}P°)	17,550	46,889	2.2E−15	2.9E−15
Fe@347.67	3d^{6}4s^2 - 3 d^6(^{5}D)4s4p (^{3}P°)	978	29,733	7.0e−16	6.9E−16
Ni@341.47	3 d^9(^{2}D)4 s -3 d^9(^{2}D)4p	205	29,481	2.9E−15	2.6E−15
Co@340.50	3p^{6}3d^8(^{3} F)4 s -3p^{6}3d^8 (^{3} F)4p	3483	32,842	3.3E−15	3.6E−15

Table 2b

TiII	configurations	E_l (cm^{-1})	E_u (cm^{-1})	σ_{SP} (cm^2)	σ_{DP} (cm^2)	σ_{cal} (cm^2)
347.72	3 d^3-3 d^2(^{3} F)4p	984	29,735	1.0E−16	6.9E−17	2.7E−16
346.16	3 d^3-3 d^2(^{3} F)4p	1087	29,968	6.1E−17	9.2E−17	2.6E−16
344.43	3 d^3-3 d^2(^{3} F)4p	1216	30,240	6.0E−17	9.8E−17	2.9E−16
350.48	3 d^2(^{1} G)4 s-3 d^2 (^{1} G)4p	15,257	43,781	1.6E−15	3.5E−15	2.8E−15
351.08	3 d^2(^{1} G)4 s -3 d^2 (^{1} G)4p	15,266	43,741	1.2E−15	3.0E−15	3.2E−15

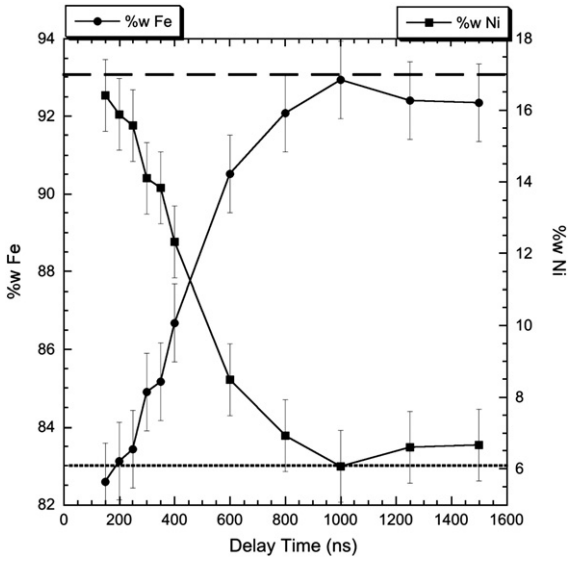

Fig. 9. Temporal evolution of Fe and Ni composition estimated by Eq. (20), corrected by the atomic weight. Dashed and dotted lines indicate the composition value of Fe and Ni, respectively, as reported in Ref. [28].

not negligible difference from the numerical point of view. This condition would allow eliminating partially the dependence on temperature from Eq. (19) because the exponential term would converge to 1 and so:

$$\frac{N_0^X}{N_0^Y} = \frac{I_{ul}^X \lambda_{ul}^X \sigma_{l'u'}^Y \nu(E_{u'l'}) g_{l'}^Y Z^X(T)}{I_{u'l'}^Y \lambda_{u'l'}^Y \sigma_{lu}^X \nu(E_{ul}) g_l^X Z^Y(T)} = R_{X/Y} \tag{20}$$

Considering a sample containing n elements, whose cross sections have been previously determined or calculated, a system of n-equations, including the closure equation proposed in Ref. [27], can be obtained:

$$\begin{cases} \dfrac{N_0^{X1}}{N_0^{Xn}} = R_{X1/Xn} \\ \dfrac{N_0^{X2}}{N_0^{Xn}} = R_{X2/Xn} \\ \cdots\cdots\cdots\cdots \\ \dfrac{N_0^{Xn-1}}{N_0^{Xn}} = R_{Xn-1/Xn} \\ \sum_i^n N_0^{Xi} PA_i = 100 \end{cases} \tag{21}$$

In order to avoid the correction due to the contribution of the ionized fraction of each element Xi, evaluated by the Saha equation, a suitable delay time should be chosen. Fig. 9 shows the result of the application of this method to the Sikhote Alin sample [28]. It can be seen that, after about 800 ns, the measured atomic concentration converges to the element concentration in the target, marked by lines in the figure.

The method has been applied to three different iron meteorites previously analyzed by traditional CF-methodology in Refs. [12, 13]. In these experiments, carried out in different conditions (operator, laser fluence between 6 and 30 J cm^{-2}, target positioning), a laser pulse at 532 nm has been employed, while the used cross sections have been determined with a 355 nm laser pulse experiment as described in the previous section.

Table 3 collects the results of the elemental analysis obtained by Eq. (21), i.e., based on cross section determination, together with those available in the literature and those obtained by traditional free calibration (CF) [27] based on Boltzmann distribution [12, 13]. The results show an acceptable agreement, especially keeping in mind that the concentration of minor elements can slightly differ point by point in the sample [13] and that literature data represents an average value in one gram of sample [28].

It would be interesting to underline that in the case of Co, the classical approach based on upper level population and Boltzmann distribution requires the excitation temperature, which appears in the following equation:

$$\frac{N_0^X}{N_0^Y} = \frac{I_{ul}^X \lambda_{ul}^X A_{u'l'}^Y g_{u'}^Y Z^X(T)}{I_{u'l'}^Y \lambda_{u'l'}^Y A_{ul}^X g_u^X Z^Y(T)} \exp\left(\frac{E_u^X - E_{u'}^Y}{kT}\right) \tag{22}$$

In this specific case, comparing Eqs. (20) and (22), the advantage of the approach discussed in this work can be appreciated. Theoretically, Eq. (20) and (22), which are based on opposite approaches, should give the same result. In fact, the first one describes the forward excitation process and the second one the backward emission decay, but, practically, Eq. (20), in the example of Co, does not requires a precise value for the excitation temperature and the Boltzmann distribution for calculating the exponential term. Of course, a rough estimation of the temperature is still required for the calculation of the partition function, but in this case the value of temperature is not so critical. As an example, the ratio of the partition functions of Fe I and Ni I in the range of temperature between 6000 K and 10,000 K varies from 1.1 to 1.4, while the corresponding exponential term varies 2.5 times faster.

It is also worth emphasizing that the cross section value to be used in this method does not need to be determined by LIBS, but can be

Table 3
Elemental composition of irony meteorites (Sikote Alin, Toluca, Campo del Cielo) determined with the method described in present work compared with the results obtained with a traditional CF procedure and literature values [12, 13].

	Present work			Literature [28]			CF [12,13]		
	Fe	Ni	Co	Fe	Ni	Co	Fe	Ni	Co
Sikote Alin	93.0	6.3	0.8	93.5	6.0	0.48	94.0	5.7	0.6
Toluca	92.3	6.9	0.8	91.5	8.2	0.45	92.0	7.1	0.35
Campo del Cielo	93.1	6.2	0.5	92.6	6.9	0.50	91.0	8.0	0.7

obtained by other experimental techniques (LIF, electron scattering etc.) or by theoretical calculation as well.

As an example, we report here the determination of Pb and Cu composition in a set of copper based alloys. In this case the values of cross sections, for the spectral lines of Pb I at 280.2 nm ($E_l = 10650\ cm^{-1}$ and $E_u = 46329\ cm^{-1}$) and Cu I at 282.4 nm ($E_l = 11203\ cm^{-1}$ and $E_u = 46598\ cm^{-1}$), have been calculated directly by Eq. (17) and then, Eq. (21) have been applied to a set of measurements on 4 bronze samples labeled L3, B4, B21 and B22 as described in Ref. [14]. The samples have been irradiated with a 1064 nm laser pulse at an estimated fluence of 45 J cm^{-2}. The resulting analysis is reported in Fig. 10 together with the certified values: it can be seen that an acceptable agreement was obtained for all samples.

In the latter case of study, where the lower and upper levels have the same energy, there is no difference using either of Eq. (20) or Eq. (22) because in both expressions the exponential term containing the temperature converges to 1.

When the energy levels of the transition are characterized by similar values, it is easy to see that combining Eqs. (20) and (22) the following equality is obtained:

$$\frac{\sigma^Y_{l'u'} g^Y_{l'}}{\sigma^X_{lu} g^X_l} = \frac{A^Y_{u'l'} g^Y_{u'}}{A^X_{ul} g^X_u} \tag{23}$$

Calculating the two members of Eq. (23) independently by Eq. (17) and using literature data [25], exactly the same value (0.062) is indeed obtained. This result is the obvious consequence of the fact that both the excitation cross section (see Eq. (17)) and the emission coefficient [6,10] are proportional to the oscillator strength.

5. Conclusion

In this paper the LIP features have been investigated by taking into consideration elementary processes. A scenario has been depicted where the emission decay compensates the loss of slow electrons due to recombination in the balance between electron impact excitation/de-excitation. This hypothesis allows estimating the electron impact cross section for optical allowed transition. Whereas this estimation of the cross section cannot be considered an accurate method for the real determination of the cross section energy function, it allows to unequivocally connecting the emission intensity to the excitation binary collision, irrespective of the experimental conditions. When the cross section values have been estimated, these data can be used for LIBS elemental analysis.

This approach can be applied to calibration-free analysis and, although is not so accurate as the classical calibration curve method, it allows obtaining the concentration of element directly by the corresponding peak intensity. Further studies for the application of this methodology are in progress. Even when taking into consideration the assumption made, in particular these related to the spatial inhomogeneity of the plasma, the preliminary results shown in this paper look indeed promising.

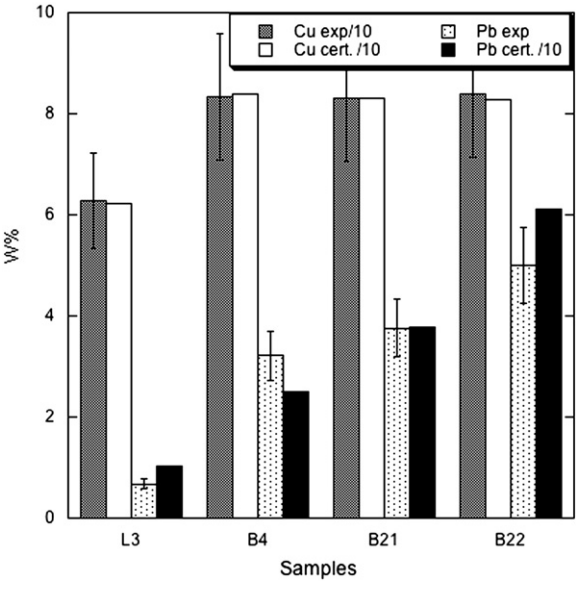

Fig. 10. Experimental results of LIBS analysis of Cu and Pb by the method described in the present paper compared to certified values for a set of copper based alloys. Delay time: 1 μs; gate width: 5 μs; laser pulse fluence of 45 J cm^{-2} at 1064 nm.

Acknowledgments

The author would like to thank Dr G. Colonna, Dr A. Laricchiuta, Dr M. Dell'Aglio and Dr R. Gaudiuso from CNR-IMIP for taking part in the scientific discussion, and Prof M. Capitelli and Prof. S. Longo from the University of Bari and Prof. N. Omenetto from the University of Florida for precious suggestions in the development of this work.

References

[1] L.J. Radziemski, D.A. Cremers (Eds.), Laser-induced plasma and applications, Marcel Dekker, New York, 1989.
[2] D.W. Hahn, N. Omenetto, Laser-induced breakdown spectroscopy (LIBS), part I: Review of basic diagnostics and plasmaparticle interactions: Still-challenging issues within the analytical plasma community, Appl. Spectrosc. 64 (2010) 335A–366A.
[3] E. Tognoni, G. Cristoforetti, S. Legnaioli, V. Palleschi, Calibration free Laser Induced Breakdown spectroscopy: State of the art, Spectrochim. Acta Part B 65 (2010) 1–14.
[4] N. Konjevic, Plasma broadening and shifting of non-hydrogenic spectral lines: present status and applications, Phys. Rep. 316 (1999) 339–401.
[5] M. Capitelli, F. Capitelli, A. Eletskii, Non-equilibrium and equilibrium problems in laser-induced plasmas, Spectrochim. Acta Part B 55 (2000) 559–574.
[6] G. Cristoforetti, A. De Giacomo, M. Dell'Aglio, S. Legnaioli, E. Tognoni, V. Palleschi, N. Omenetto, Local Thermodynamic Equilibrium in Laser-Induced Breakdown Spectroscopy: Beyond the McWhirter Criterion, Spectrochim. Acta Part B 65 (2010) 86–95.
[7] J.A.M. Van der Mullen, Excitation equilibria in plasmas; a classification, Phys. Rep. PRPLCM 191 (2 & 3) (1990) 109–220.
[8] A.W. Miziolek, V. Palleschi, I. Schechter (Eds.), Laser Induced Breakdown Spectroscopy, Cambridge University Press, 2006, Chapter 1.
[9] D. Pietanza, G. Colonna, A. De Giacomo, M. Capitelli, Kinetic Processes for Laser Induced Plasma Diagnostic: a Collisional-Radiative Model Approach, Spectrochim. Acta Part B 65 (2010) 616–626.
[10] H.R. Griem, Validity of local thermal equilibrium in plasma spectroscopy, Phys. Rev. 131 (1963) 1170–1176.
[11] A. De Giacomo, M. Dell'Aglio, D. Bruno, R. Gaudiuso, O. De Pascale, Experimental and theoretical comparison of Single-pulse- and Double-pulse-LIBS on metallic samples, Spectrochim. Acta Part B 63 (2008) 805–816.
[12] A. De Giacomo, M. Dell'Aglio, O. De Pascale, S. Longo, M. Capitelli, Laser Induced Breakdown Spectroscopy on meteorites, Spectrochimica. Acta Part B 62 (2008) 1610–1615.
[13] M. Dell'Aglio, A. De Gaicomo, R. Gaudiuso, O. De Pascale, G.S. Senesi, S. Longo, Laser Induced Breakdown Spectroscopy applications to meteorites: Chemical analysis and composition profiles, Geochim. and Cosmochim. Acta 74 (2010) 7329–7339.
[14] A. De Giacomo, M. Dell'Aglio, R. Gaudiuso, O. De Pascale, Laser Induced Breakdown Spectroscopy methodology for the analysis of copper-based-alloys used in ancient artworks, Spectrochim. Acta Part B 63 (2008) 585–590.
[15] G. Colonna, L.D. Pietanza, M. Capitelli, Coupled Solution of a Time-dependent Collisional-Radiative Model and Boltzmann Equation for Atomic Hydrogen Plasmas: Possible Implications with LIBS Plasmas? Spectrochim. Acta Part B 56 (2001) 587–598.
[16] A. De Giacomo, R. Gaudiuso, M. Dell'Aglio, A. Santagata, The role of Continuum radiation in Laser Induced Plasma Spectroscopy, Spectrochim. Acta Part B 65 (2010) 385–394.
[17] B. Makin, J.C. Keck, Variational theory of three-body electron-ion recombination rates, Phys. Rev. Lett. 11 (1963) 281–283.
[18] L.D. Landau, E.M. Lifshitz, Theoretical Physics, vol. 4, Pergamon, 1971 section 56.
[19] K. Hassouni, F. Silva, A. Gicquel, Modelling of diamond deposition microwave cavity generated plasmas, J. Phys. D: Appl. Phys. 43 (2010) 153001.
[20] H.R. Griem, Principles of Plasma Spectroscopy, Cambridge University Press, 1997.
[21] H.R. Griem, Spectral Line Broadening by Plasmas, Accademic Press, New York, 1974.
[22] http://www-amdis.iaea.org/ALADDIN, consulted in January 2011.

[23] J.D. Hey, Criteria for local thermal equilibrium in non-hydrogenic plasmas, J. Quant. Spectrosc. Radiat. Transfer 16 (1976) 69–75.
[24] http://www.nist.gov, consulted in January 2011.
[25] http://www.pmp.uni-hannover.de/cgi-bin/ssi/test/kurucz/sekur.html, consulted in January 2011.
[26] J. Hermann, A.L. Thomann, C. Boulmer-Leborgne, B. Dubreuil, M.L. De Giorgi, A. Perrone, A. Luches, I.N. Mihailescu, 2928–2936, Plasma diagnostic in pulsed laser TiN layer deposition, J. Appl. Phys. 77 (1995) 2928–2936.
[27] A. Ciucci, M. Corsi, V. Palleschi, S. Rastelli, A. Salvetti, E. Tognoni, New Procedure for Quantitative Elemental Analysis by Laser-Induced Plasma Spectroscopy, Appl. Spectrosc. 53 (1999) 960–964.
[28] J.T. Wasson, H. Huber, D.J. Malvin, Formation of IIAB iron meteorite, Geochim. Cosmochim. Acta 71 (2007) 760–781.